FIRE AND MATERIALS
Fire Mater. 2017
Published online in Wiley Online Library (wileyonlinelibrary.com). DOI: 10.1002/fam.2418

Mass loss and flammability of insulation materials used in sandwich panels during the pre-flashover phase of fire

A.W. Giunta d'Albani[1], L.L. de Kluiver[1], A.C.J. de Korte[1,*,†], R.A.P. van Herpen[1,2], R. Weewer[3] and H.J.H. Brouwers[1]

[1]*Department of the Built Environment, Eindhoven University of Technology, 5600 MB Eindhoven, The Netherlands*
[2]*Nieman Raadgevende Ingenieurs, Zwolle, Overijssel 8004 DC, The Netherlands*
[3]*Instituut Fysieke Veiligheid, Arnhem, Gelderland 6801 HA, The Netherlands*

SUMMARY

Nowadays, buildings contain more and more synthetic insulation materials in order to meet the increasing energy-performance demands. These synthetic insulation materials have a different response to fire. In this study, the mass loss and flammability limits of different sandwich panels and their cores (polyurethane (PUR), polyisocyanurate (PIR) and stone wool) are studied separately by using a specially designed furnace. Expanded polystyrene and extruded polystyrene are tested on their cores only. The research has shown that the actual mass loss of synthetic and stone wool-based cores is comparable up to 300 °C. From 300 °C onwards, the mass loss of PUR panels is significant higher. The mass losses up to 350 °C are 7%, 29% and 83% for stone wool, PIR and PUR respectively, for the influenced area. Furthermore, delamination can be observed at exposure to temperatures above 250 °C for the synthetic and 350 °C for the mineral wool panels. Delamination occurs due to the degradation of the resin between core and metal panels and the gasification of the (PUR) core. The lower flammability limits have been established experimentally at 9.2% m/m (PUR) and 3.1% m/m (PS). For PUR, an upper limit of 74% was found. For PIR and mineral wool, no flammability limits could be established. Copyright © 2017 John Wiley & Sons, Ltd.

Received 14 February 2015; Revised 24 September 2016; Accepted 16 November 2016

KEY WORDS: flammability limits; mass loss; sandwich panels; insulation materials; pre-flashover phase; fire safety engineering

1. INTRODUCTION

Nowadays, buildings contain more and more synthetic insulation materials in order to meet the higher demands for energy performance. These synthetic insulation materials have a different response to fire compared with mineral insulation materials, like stone wool. The focus in this study is on the pre-flashover phase of fire (up to 400 °C) because this is the phase in which the fire brigade is still able to intervene inside the fire compartment (offensive fire attack). This is carried out in order to evaluate the risk of smoke gas explosions during a real fire. Smoke gas explosions can occur even before flash over due to the release of combustible pyrolysis gases when the proper mixture of gases with air exists even at lower temperatures. This causes a major risk for fire fighters entering the fire compartment for internal fire fighting.

*Correspondence to: A. C. J. de Korte, Department of the Built Environment, Eindhoven University of Technology, PO Box 513, 5600 MB Eindhoven, North Brabant, The Netherlands.
†E-mail: a.c.j.dekorte@gmail.com

Furthermore, here, the focus is on sandwich panels and their synthetic insulation cores. A sandwich panel consists of a core that has a high insulation capacity, wrapped in facings that are often made of thin sheets of steel or aluminium, but other materials like wood, plastics or paper are also possible. Sandwich panels for external roof and wall applications are, in approximate order of frequency of use, polyurethane (PUR), polyisocyanurate (PIR), Loss Prevention Certification Board-approved PIR, stone fibre (mineral), expanded polystyrene (EPS) and glass fibre (mineral), while for internal use, these are EPS, extruded polystyrene (XPS), PUR, PIR, rock fibre, modified phenolic foam and cellular glass insulation [1].

This paper focuses on five different insulation materials, namely stone wool, PUR, PIR, EPS and XPS, of which the properties are described in Section 2. These materials can be applied as a core for sandwich panels, as well as single insulation material. Of these materials, stone wool is considered as incombustible, while the other materials are, in general, classified as combustible. Another main difference between both categories is organic versus inorganic chemical background. Inorganic fibrous materials represent 60% v/v of the European market for insulation materials, while organic foamy materials, like EPS, XPS and PUR, account for 27% v/v of the market [2]. The other 13% v/v consist of combined materials (such as siliconated calcium, gypsum foam and wood–wool) and new technology materials (such as transparent materials and dynamic materials) [2]. For sandwich panels, the figures are different. Exact numbers are not available, but it is known that sandwich panels with EPS and XPS are hardly applied in the Netherlands. Still, the flammability of EPS and XPS is relevant because EPS/XPS occupies 35% of the market for flat roofs in the Netherlands [3].

For this study, the mass loss and flammability of pyrolysis gases are of interest and are experimentally determined. Flammability is both scenario (temperature and fire growth rate) and material dependent [4, 5]. Flammability is determined in this paper for the complete mixture of fire effluents rather than for individual gases, which is usual for chemical analysis. The fire effluent due to the thermal decomposition of both synthetic and natural polymers contains a complex mixture of chemicals which will always contain irritating as well as asphyxiating agents [6].

The application of sandwich panels with combustible cores introduces the following fire hazards: delamination of steel faces [7] due to decomposition of the resin between panel and core as well as due to thermal stresses and expansion [8], the possibility for pyrolysis gases to travel through panel to other compartments due to panel distortion and the opening of the joints between the panels [8], the possibility that the core can be on fire unnoticed and flames are spread through the core [9], the presence of dense smoke caused by the pyrolysis of the insulation core [8] and the possibility of smoke gas explosion of the mixture of pyrolysis gases and hot air. Figure 1 shows graphically the temperature ranges at which EPS, PUR, PIR and wood melt, pyrolyse and ignite. This paper aims to provide insight in the possible hazard of a smoke gas explosion due to combustible mixtures formed during the pre-flashover phase ($<$400 °C) because in this phase, the fire brigade still is able to intervene inside.

2. LITERATURE REVIEW

In this section, a short literature review on the fire behaviour of various insulation materials will be given with a focus on the pre-flashover phase. The burning of an organic material, such as a polymer, is a complex process, in which volatile breakdown products react to some extent with oxygen, producing a cocktail of products, consisting of carbon dioxide (CO_2) and water and a mixture of a variety of products of incomplete combustion [10]. The last category has influence on the flammability of the fire effluent. The flammability range is the range between the lower and upper limit in which a mixture of pyrolysis gases and air can ignite [11]. The lower (lowest amount of pyrolysis gases) and upper (highest amount) limits depend on the composition of the cocktail of products of the thermal degradation process and the temperature. The composition of this cocktail of fire gases depends on the decomposing materials and on oxygen supply, temperature and fire growth rate [5,12].

DOI: 10.1002/fam

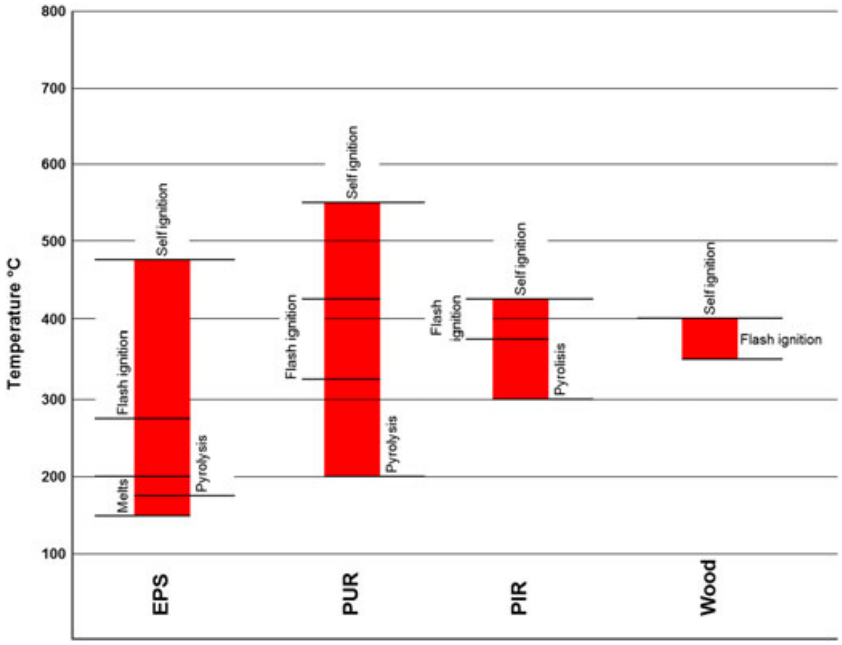

Figure 1. Schematic representation of the ignition temperatures of the different insulation materials based on Cooke [7]. [Colour figure can be viewed at wileyonlinelibrary.com]

2.1. Polyurethane

Polyurethanes are complex and extremely large polymers with repeating urethane groups/linkage, which are produced by the reaction between isocyanate (—N═C═O) with compounds which at least contain two active hydrogen atoms [13]. Besides the urethane linkages, a PUR foam may also contain aliphatic and aromatic hydrocarbons, esters, amides, disubstituted urea, biuret, allophanate, isocyanurate, uretidione and carbodiimide groups [14]. Due to the possible presence of these compounds, a large number of PUR foams with different properties exist. Table I shows the dissociation temperatures of the different chemical linkages in PUR, which influence the thermal stability of the PUR. Singh and Jain [14] gave a comprehensive literature overview of the influences on ignition, combustion, toxicity and fire retardancy of the addition of different compounds to PUR. Chattopadhyay and Webster [13] gave an overview of the thermal degradation processes of PUR materials. In this section, the focus is on rigid PU foams, which are applied in the construction sector.

Jiao *et al*. [15] performed thermogravimetry (TG) and differential scanning calorimetry (DSC) on rigid PU foams in nitrogen (N_2) and air at a heating rate of 10 °C/min. They found two-stage and three-stage thermal degradation processes in N_2 and air atmospheres respectively. In both atmospheres, a small amount of mass loss (~3%) was observed between 100 and 190 °C, which were explained by the evaporation of moisture. The second peak was found at 340 and 314 °C for

Table I. Dissociation temperatures of the different chemical linkages, which are common in polyurethane (PUR) and polyisocyanurate (PIR) [14].

Linkage	Dissociation temperature (°C)
Allophanate	100–120
Biuret	115–125
Urea	160–200
Urethane	180–200
Disubstituted urea	235–250
Carbodiimide	250–280
Isocyanurate	270–300

DOI: 10.1002/fam

N_2 and air respectively, which is the main degradation stage. Furthermore, they concluded that the whole process in air is accelerated due to the presence of oxidizing gases.

Jiao *et al*. [16] gives the mass loss for three temperature ranges by using TG under N_2 atmosphere. The mass loss during the first stage (71–234 °C) was 11.6%. The second stage (234–400 °C) leads to a mass loss of 50.1%, while the third stage from 400 to 600 °C leads to 10.3% mass loss. Furthermore, a mass spectrometry was performed by Jiao [16], showing the presence of CO_2 (peaks at 250 and 450 °C) and C_2H_4O (peak at 350 °C) and absence of hydrogen cyanide.

The possible fire effluents produced from PUR are CO_2, carbon monoxide, nitrogen oxides, ammonia, benzene, acetaldehyde, alkenes, hydrogen cyanide, toluene, hydrogen fluoride, hydrogen chloride, hydrogen bromide and phosgene [17]. In Table II, the flammability limits for some of these effluents can be found, as given by the Matheson gas data book [18].

2.2. Polyisocyanurate

The main difference between PUR and PIR is the presence of a high amount of isocyanurate ring structures in the latter, which are created by the trimerization of three molecules of the polymetric isocyanate [19]. Pure polyisocyanurate foams have a high friability, which limits the practical application of pure PIR foams. Therefore, urethane and isocyanurate linkages are often combined in foams. The urethane component in the material provides the desired physical properties, while the isocyanurate component provides the required flame retardancy [20]. The urethane linkage dissociates at approximately 200 °C, while polyisocyanurate linkage breaks at around 350 °C [17,21]. This difference was also observed by Dick *et al*. [22] during the DSC of several foams with different amounts of urethane and isocyanuate linkages. The ratio isocyanate/polyol (NCO/OH) plays an important role in determining the structure and thermal properties of PIR-based foams because it controls the relative amounts of urethane and isocyanurate linkages [22]. Zhang *et al*. [23] show that the onset temperature of the mass loss and stability at high temperature increased with increase of the molar ratio of NCO/OH. Gao *et al*. [24] found that increasing isocyanurate index will decrease the polyol release (the major volatile product), and it will increase the CO_2 release (a product of the isocyanurate decomposition).

Dick *et al*. [22] have performed thermogravimetric analysis (TGA) test in air and inert (N_2) environment. They noticed a plateau of stability between 350 and 500 °C in the degradation under air. They also noticed two major decompositions or debonding processes occurring within the

Table II. Flammability ranges of some fire effluents, which may be present during the degradation of polyurethane (PUR), polyisocyanurate (PIR), polystyrene (PS) and phenolic resin [18] (not all effluents are present in each material).

Gas		Present in				Lower flammability limit %v/v	Upper flammability limit %v/v
		PUR	PIR	PS	PH		
Acetylene	$H-C\equiv C-H$			X		2.6	13.0
Acetaldehyde	CH_3CHO	X	X			4.0	60.0
Ammonia	NH_3	X	X			15.0	28.0
Benzene	C_6H_6	X	X	X		1.3	7.9
Carbon monoxide	CO	X	X			12.0	74.0
Ethane	C_2H_6			X		3.0	12.4
Ethyl benzene	$C_6H_5CH_2CH_3$			X		1.0	6.7
Ethylene	$H_2C=CH_2$			X		2.7	36.0
Hydrogen cyanide	$H-C\equiv N$	X	X			5.6	44.0
Methane	CH_4			X		5.0	15.0
Naphthalene	$C_{10}H_8$				X	0.9	5.9
Styrene	$C_6H_5CH=CH_2$			X		1.1	100.0
Toluene	$C_6H_5-CH_3$	X	X	X		1.2	7.1
Xylene	C_8H_{10}				X	0.9	5.9

DOI: 10.1002/fam

polymer. The low-temperature process (around 315 °C) is breaking the urethane linkages, and the higher-temperature process is breaking the isocyanurate linkages (around 450 °C).

Vitkauskiene *et al*. [17] produced several PIR foams based on polyethylene terephthalate-derived aromatic polyester polyols and compared these with a PIR based on commercially available aromatic polyester polyols based on terephthalic acid. During the TGA of the PIR, they found two main peaks. The first peak between 190 and 240 °C was related to the evaporation of flame retardant Tris (1-chloro-2-propyl) phosphate and leads to a mass loss of 8–10%. The second peak was around 330 °C with a mass loss of around 30%.

2.3. Expanded polystyrene

Expanded polystyrene is a thermoplastic that melts when heated. Polystyrene products burn vigorously and produce large quantities of black smoke, even after the addition of flame retardants [19]. The melting of polystyrenes will introduce the risk of (flaming) droplets during a fire, which can be a hazard for the fire department. Baker [25] describes the chemical and physical aspects of the degradation process of EPS. EPS softens above 80 or 90 °C, depending on the duration of exposure to these temperatures. Until approximately 150 °C, the EPS will shrink and return to its original density as a solid polystyrene. When heating further, EPS will melt to a liquid and start forming gas above 200 °C. These gases can be ignited at temperatures between 360 and 380 °C, and self-ignition occurs at approximately 500 °C [25]. Griffin *et al*. [9] found a three-stage degradation process of EPS during heating in air. According to Griffin *et al*., the first two stages occur between 275 and 375 °C, while the third stage occurs between 350 and 450 °C under heated air atmosphere. EPS has a two-stage decomposition in an N_2 environment [16]. The first small peak under N_2 atmosphere is visible around 120 °C and does not lead to clear mass loss. The second stage (under N_2) between 377 and 417 °C leads to a mass loss of 78.7%, and a heat absorption of 2807 J/g is associated with this stage [15]. The temperature of the second stage in N_2 mentioned by Jiao [16] is in line with the findings of Griffin *et al*. [9]. EPS is a hydrocarbon $(H_8C_8)_n$ which decomposes in the end into CO, CO_2 and H_2O [26]. Jiao *et al*. [16] gives the most important intermediate products, which are shown in Table III. Although the final products are not flammable, some intermediate products are flammable (Table IIIa). Gurman *et al*. [27] mentioned the presence of obligomers of styrene (dimer and trimer), toluene, benzene, ethylbenzene and α-methylstyrene, benzaldehyde and benzoic acid during the thermal degradation of polystyrene.

Table III. The most flammable gases in effluent when heating (a) expanded polystyrene (EPS) and (b) extruded polystyrene (XPS) according to Jiao *et al*. [16].

Temperature (°C)	Mass-to-charge ratio (m/z)	Volatile fragment
(a)		
	12.28	CO
	17.18	OH, H_2O
	27	C_2H_3
	29	C_2H_5
350.400–420	44	CO_2
	45	CH_3CH_2O, CH_3CHOH
	46	CH_3CH_2OH, $H_2O + C_2H_4$
	51.52	C_4H_3, C_4H_4
(b)		
	12	C
	17.18	OH, H_2O
	27	C_2H_3
	29	C_2H_5
470	44	CO_2
400–450	51.52	C_4H_3, C_4H_4
425–475	65.66	C_5H_5, C_5H_6
425–475	74	

DOI: 10.1002/fam

2.4. Extruded polystyrene

Extruded polystyrene means that the base material is the same as of EPS, but the production method differs. XPS is produced by a continuous extrusion process, where blowing agents are added to produce a close cell material. Jiao *et al*. [16] gives a two-stage thermal decomposition in an N_2 atmosphere. The first stage (228–298 °C) has a mass loss of 7.10%. The second stage (342–456 °C) leads to a mass loss of 87.6%, and the performed DSC shows a heat absorption peak of 1153 J/g. Table IIIb shows the most flammable gases in the fire effluent when heating XPS.

2.5. Mineral (stone) wool

Mineral wool products such as glass and stone wool are inorganic materials. The mineral wool itself can be considered as thermally stable because it can be applied up to 600 °C [28]. It is often referred to as incombustible because it is graded as a Class A material according to European 13501-1 standard, which is the class with the highest fire resistance.

The main components of stone wool are amphibolites (85% m/m), limestone (<6% m/m) and a variety of calcium oxides (<9% m/m). Stone wool fibres are produced by melting this mixture and centrifuging this melted mixture in a cylindrical tank with microscopic holes on the outer surface. The melted mixture which escapes through these holes is cooled by ambient air and becomes solid-forming fibres [28] with a thickness of 5–10 μm [29].

The next step is mechanically compressing the fibres to form compressed plates. In order to keep the fibres together in the plate, a resin is injected. This resin hardens at a temperature of 250 °C, giving the board its strength [28]. The resin used in mineral wool boards is typically an urea-phenol-formaldehyde-based solution [30], and the amount is typically around 1–2% m/m [31]. Balcerowiak *et al*. [30] performed a research to thermal stability of phenol-formaldehyde-urea binder, which shows that the temperature of thermal stability decreases with exposure time, from 250 °C at short exposure (1 min) to 190 °C at long exposure (200 min).

Furthermore, when applying mineral wool in sandwich panels, a resin is used to stick the skins to the core of the panels, which can be combustible as well. In Table II, the flammability limits for some of the effluents of a phenolic resin [32] can be found, as given by the Matheson gas data book [18].

3. EXPERIMENTAL SETUP

3.1. Test setup

Two different series of experiments were carried out in this study, (1) the mass loss and (2) the flammability experiment. Both experiments used the same basic furnace (Section 3.1.1) with some further specified modification, which are described in Sections 3.1.2 and 3.1.3 respectively.

3.1.1. The basic furnace (test setup). The furnace (Figure 2) has an inner space of 30 × 30 × 60 cm (l * w * h) and is built with autoclaved aerated gas concrete blocks. These blocks were covered with aluminium foil to decrease the absorption of pyrolysis gases by the gas concrete blocks and to create acceptable air tightness. The heating of the furnace is carried out by a large electric heating element of 2300 W. This basic setup can be used for both the mass loss (Section 3.1.2) and flammability experiments (Section 3.1.3). The heating of the samples is carried out by an electronic heating element in order to minimize the influence on the composition of gases by possible unburnt fuels. Gas burners would influence the composition of fire effluent. The heating element is made out of solid brass plates, 20 × 30 cm, in which three heating threads of 800 W are placed. Due to its size, the samples will be equally exposed to the radiation. The heating element is connected to a sheet thermocouple that has been placed at the front side of the furnace, just below the surface of the frame in which the sample is placed. This position allows determining the temperature at the height of the sample without blocking a part of the sample.

DOI: 10.1002/fam

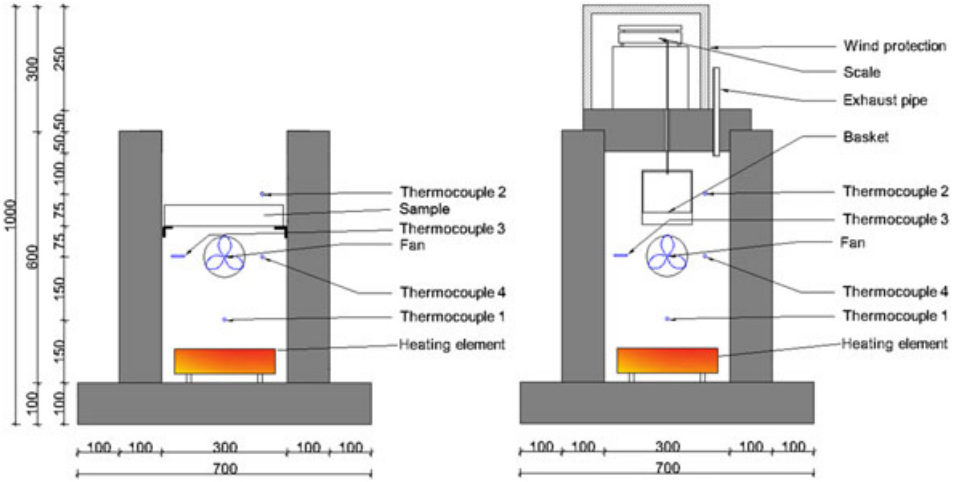

Figure 2. Drawing of the basic furnace with at the left the setup for the mass-loss experiment and at the right the setup for the flammability experiment. [Colour figure can be viewed at wileyonlinelibrary.com]

The heat element is controlled by this sheet thermocouple which is attached to the self-adjusting temperature controller type West 6100.

3.1.2. Mass-loss experiment. The mass loss experiment uses three different constant temperatures to which the samples are exposed at 150, 250 and 350 °C. The temperature 150 °C has been chosen as lower limit because degradation of the adhesive layers starts at around 150 °C; the upper limit has been set at 350 °C. This temperature corresponds to the temperature to which a fire fighter can be safely exposed. This corresponds to radiation flux of 4.5 kW/m^2 for a duration of 20 min with a view factor of 0.5. This radiation flux is given by Australasian Fire and Emergency Service Authorities Council [33].

The sample is placed in a sample tray. This sample tray has dimensions of 29.8 × 29.8 cm made out of L-steel profile 50 * 50 * 5 mm and a mass of 4.133 kg and is supported by L-steel profiles, which are mounted to the sides of the furnace. The samples are insulated with ceramic insulation to prevent heat transfer through the sides of the sample. In order to create a realistic situation for the mass-loss experiment, the top part of the furnace needs to be open, so the 'outside' of the sample is exposed to ambient temperatures while being exposed to heat within the furnace. It is the authors' opinion that by exposing the samples to a hot layer of air combined with the radiation of the brass element from below and ambient temperatures from above, a realistic scenario is simulated. Figure 3 shows a photo of a sample in the furnace. Furthermore, the experiments are performed three times to verify repeatability of the experiment.

3.1.3. Flammability experiment. For the flammability experiment, the same basic furnace setup is applied as from Section 3.1.1. Unlike the mass-loss experiment, the experimental setup for flammability experiment was closed by using a lid. Another difference is that the sample is placed in a bucket in the middle of the furnace and its mass is measured continuously by a scale on top of the furnace. Besides that, the flammability experiment uses an increasing temperature from 150 until 400 °C, while three fixed temperatures are applied during the mass-loss experiment. The experiment was also used to validate the furnace by using thermogravimetric analysis data from literature. The results from the continuous measurement of the sample mass during the experiment were compared with TGA data. The results are further discussed in Section 4.1.1.

The flammability itself is tested outside the furnace by using an exhaust pipe. Three different ways to ignite the gases were applied, namely piezoelectric element, regular lighter and glass bottle with lighter. The glass bottle method uses a glass bottle to capture the gas mixture from the exhaust, and the gas mixture is then ignited with regular lighter.

The flammability limit (τ) is the mass-based ratio of mass of the pyrolysis gases (m_p) on total mass of gases (the air flow, m_t) present.

DOI: 10.1002/fam

Figure 3. A sample in the furnace during the mass-loss experiment while exposed to the heat from below. [Colour figure can be viewed at wileyonlinelibrary.com]

$$\tau = \frac{m_{\mathrm{p}}}{m_{\mathrm{t}}} \tag{1}$$

The mass of the pyrolysis gases is calculated based on the measured mass loss of the sample. Because the mass flow of air cannot be measured directly, this will be calculated by using the ideal gas law. The assumption is that the pressure in the furnace remains equal to the outside pressure due to the exhaust, assuming that the capacity of the exhaust is high enough to cope with the mass flows. Some preliminary calculations have been performed, which indicates that the capacity of exhaust is sufficient. Using the ideal gas law with an isobaric process, the change in volume equals

$$\Delta \mathrm{V} = \left(V_1 \cdot \frac{T_2}{T_1}\right) - V_1 \tag{2}$$

with ΔV the volume change (m^3), V_1 the volume of the oven (m^3), T_1 the temperature time step 1 (K) and T_2 the temperature time step 2 (K). The next step is to convert the volume increase to the air mass by using the density of the air. The air density is temperature dependent and reads

$$\rho = 3.46 \cdot 10^{-3} \left(\frac{p}{T}\right) \tag{3}$$

with ρ being the air density in kg/m^3, p the atmospheric pressure in Pa and T the temperature in Kelvin. The combination of Eqns (2) and (3) results in the mass flow of the air.

3.2. Materials

The tested materials are PUR, PIR, EPS, XPS and stone wool. The experiments on PUR, PIR and stone wool are performed both on the core materials (flammability experiment) and sandwich panel samples (mass loss experiment). Experiments on EPS and XPS were only carried out on the core materials because the application for sandwich panels is limited in the Netherlands [34]. Also, due to the property of EPS and XPS melting at a temperature of 150 °C, the experiments were not possible to do on PS sandwich panels because it would contaminate the furnace. Nevertheless, the flammability experiments on EPS and XPS are still relevant because both materials are applied extensively in buildings. Market figures [3] show that EPS occupies 35% of the Dutch flat roof market in 2015. This makes EPS the second most used insulation material in flat roofs in the Netherlands. PUR/PIR occupies 45%, and mineral wool occupies 16%. The remaining 4% is occupied by others. The properties of the tested samples are shown in Table IV.

DOI: 10.1002/fam

Table IV. Physical properties of the different insulation materials used in this research (fire safety class according to Eurocode [35]).

	PUR	PIR	Stone wool roof	Stone wool wall
Density (kg/m^3)	30	50	100	100
Conductivity (W/(m K))	0.023	0.023	0.041	0.042
Thickness (mm)	100/135	80/115	60/100	100
R_c value (m^{2}K/W)	4.92	4.59		
Mass (kg/m^2)	12.9	11.6	17.7	19.1
Fire safety class	B-s2,d0	B-s2,d0B-s1,d0	A1	A1

PUR, polyurethane; PIR, polyisocyanurate.

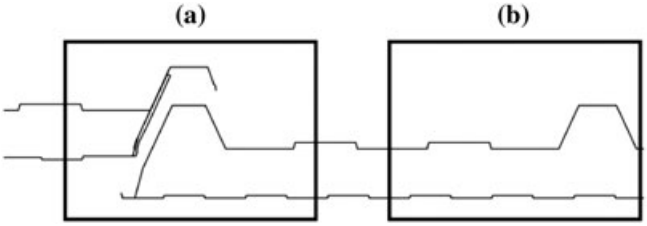

Figure 4. An example of a sample (a) with the joint between two sandwich panels and (b) without the joint between two sandwich panels.

The samples as tested during the mass loss experiment are 25 × 25 cm of which an area of 20 × 20 has been exposed to the heat source; sandwich panel samples come in two different types, namely samples with joints (in the length direction; Figure 4a) and samples without joints (Figure 4b). Figure 4 shows a cut through of a sample with joint and one without joint. The joint could be relevant because the joint could influence the mass loss and therefore the flammability of the fire effluent.

The tested samples during the flammability experiment were 10 × 10 cm, and the height of the samples was equal to the height of the core material within the sandwich panel. These samples are tested with and without the metal facing of the sandwich panels.

4. EXPERIMENTAL RESULTS

4.1. Experiments on core material samples

4.1.1. Mass loss. Table V shows the mass losses found during the flammability experiments. As one can notice from these mass losses, the temperature to which the sample was exposed is of large influence on the mass loss of the sample. While at 250 °C the mass losses were in the range up to 2%, at 400 °C, the synthetic insulation materials experience larger mass losses. PIR experienced a mass loss of 28% at 400 °C, PUR had a mass loss 44%, and both polystyrene-based materials (EPS and XPS) had a mass loss of 87%, while the stone wool experienced a mass loss of only 4% m/m. The samples of mineral wool only lose up to 4% m/m up to 350 °C, and the samples seem not to change visibly. One possible explanation of 4% m/m mass loss is the degradation of the glue. This explanation is logical because the mechanical strength of the samples is decreased during the experiment. Figure 5 shows the stone wool sample before and after heating with a weight of 5 kg on top. From this figure, one could conclude that the stone wool samples lost their compressive strength during the experiment, which most probably due to degradation of the glue, which could explain the 4% m/m mass loss of the stone wool samples.

The full results from the core sample tests regarding the mass loss and the process of the mass loss can be found in Figure 6. Figure 7 shows multiple photos of the tested sample after the test. Every

DOI: 10.1002/fam

Table V. (a) The mass loss (in mass percentage) which occurred during the flammability tests and (b) the measured ranges and derived flammability ranges (in % m/m) during flammability tests.

(a)

Materials	250 °C	400 °C
PUR	1.8%	44%
PIR	1.8%	28%
Stone wool core	0.2%	4%
Stone wool panel	0.7%	9%
Polystyrene	1.9%	87%

(b)

	LFL	UFL
PUR	9.2%	74%
PIR	> 29.2%	–
Stone wool	> 15.5%	–
Polystyrene	3.1%	–

PUR, polyurethane; PIR, polyisocyanurate; LFL, lower flammability limit; UFL, upper flammability limit.

Figure 5. Stone wool samples before (left) and after (right) mass-loss experiment with a weight of 5 kg on top. [Colour figure can be viewed at wileyonlinelibrary.com]

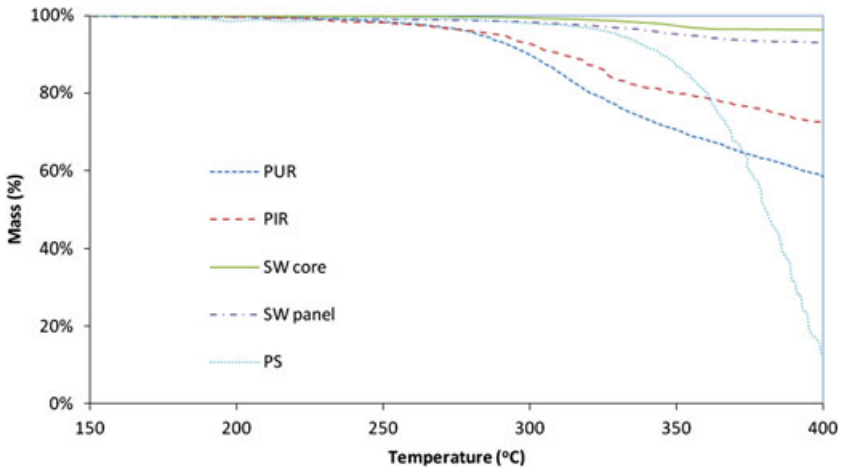

Figure 6. Mass loss of the different insulation materials during the flammability experiment. [Colour figure can be viewed at wileyonlinelibrary.com]

DOI: 10.1002/fam

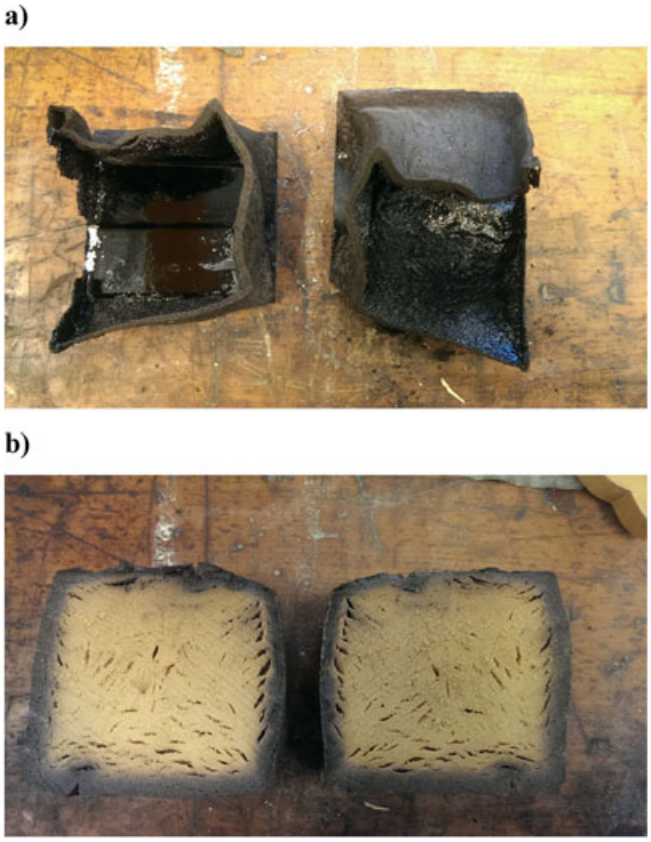

Figure 7. Cut-through of (a) polyurethane and (b) polyisocyanurate samples exposed during the flammability experiment. [Colour figure can be viewed at wileyonlinelibrary.com]

experiment was performed three times in order to verify repeatability, and the differences between the results of each experiment were minimal indeed.

From literature, the TGAs of PIR and PUR are available. These TGAs can be compared with the mass loss determined during the flammability experiment, while taking into account that the material composition of the PIR and PUR in the experiment can differ from those in the literature. Besides the chemical composition, the sample size also differs, which will never result in exact matching results. Nevertheless, the comparison is an indication of the relation between the mass loss during our experiment and the mass loss during TGA. Figures 8 and 9 show the TGAs and mass losses of

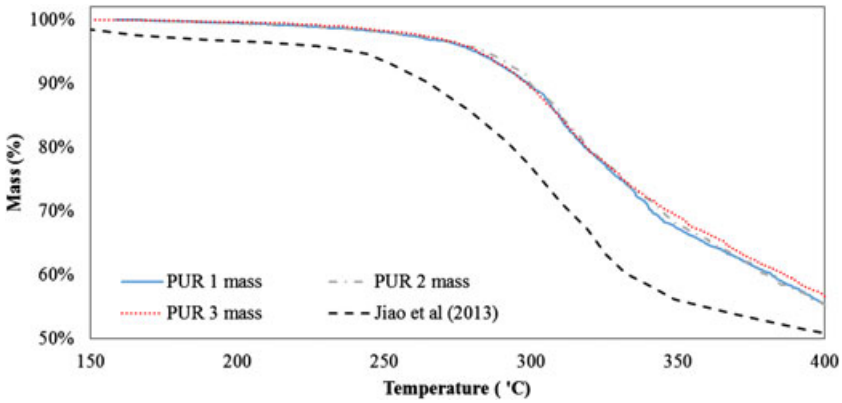

Figure 8. The mass loss of polyurethane during the flammability experiment and the mass loss in the thermogravimetric analysis measurement of Jiao *et al*. [15]. [Colour figure can be viewed at wileyonlinelibrary.com]

DOI: 10.1002/fam

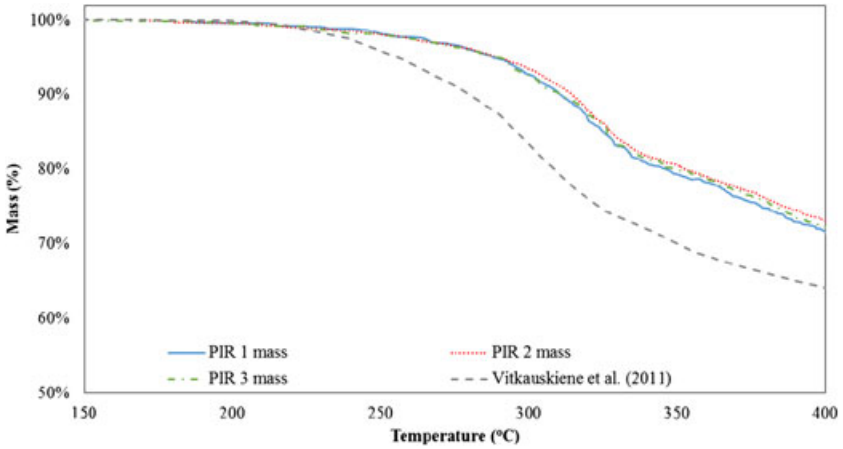

Figure 9. The mass loss of polyisocyanurate during the flammability experiment and mass loss in the thermogravimetric analysis measurement of Vitkauskiene *et al*. [17]. [Colour figure can be viewed at wileyonlinelibrary.com]

PUR and PIR respectively. The mass loss here was slower than the TGA, which could be explained by thermal inertia/slowness of the sample due to the sample size. The sample size of a TGA was few milligrams of material, while the sample size in this experiment was around 20 g of material. In the case of the latter, it took more time for the heat to reach the core of the sample. This was also visible from the cut-through photos in Figure 7. A closer review of Figures 8 and 9 shows that the start of mass loss is at the comparable temperatures and the descent is also comparable. So, the sample size seems to be of larger influence than the possible difference in composition.

4.1.2. Flammability. Table Vb shows the derived flammability limits during the experiments. The flammability limits for PIR and stone wool could not be determined during the current experiments. For PUR, a lower flammability limit (LFL) of 9.2% m/m and an upper flammability limit of 74% m/m were found. For the polystyrene materials (EPS and XPS), only the lower limit could be derived, being 3.1% for both these materials. During the current experiments, no upper limit could be established for these polystyrene materials.

In literature, the LFL given for styrene gases is 1.1% v/v [18]. Assuming that the pyrolisys gases consists of full styrene molecules, the LFL of 1,1% [v/v] equals to 2,5% [m/m]. This is close to the experimental derived value (Table V). The difference can be explained because the pyrolysis product was probably not (mono) styrene gas but contains longer chains of styrene molecules, which are more difficult to ignite. Furthermore, the temperature during the flammability experiment was low compared with the experiments in the literature, causing more difficult ignition.

4.2. Experiments on elements (sandwich and steeldeck)

4.2.1. Mass loss. The mass loss has been measured, resulting in the number as shown in Table VI and Figure 10. The mass loss of mineral wool panels showed a linear trend, while the mass loss of PIR panels slightly increased as the temperature rose. The PUR panels showed a different pattern; the mass loss increased rapidly when the temperature of 300 °C was exceeded. This leads to the assumption that the significant mass loss starts at the upper limit of this research (400 °C).

4.2.2. Intrusion depth. Due to the heat exposure of the sample to one side, the heat had to migrate through the sample, and there will be a temperature gradient across the sample. This influenced the mass loss. This caused a pattern that was similar for all the different materials. The temperature at a height of 3 cm was measured during the mass loss experiments by using a thermocouple (K3). The average intrusion depth varied between 1.52 and 1.69 cm (Table VI). If this area were taken as the influenced area, then the mass loss percentage of the material could be determined. The mass of the steel facings was not included in the calculations.

DOI: 10.1002/fam

Table VI. The mass loss (in gram) and the intrusion depth of the degradation front and mass loss percentage at 350 °C during the mass loss test.

Core type		PIR	PUR	Stone wool wall	Stone wool roof
Mass loss (g)	150 °C	1.72	1.05	1.17	1.78
Mass loss (g)	250 °C	2.4	3.32	2.3	2.45
Mass loss (g)	350 °C	8.92	15.12	5.22	4.63
Intrusion depth (cm)		1.61	1.52	1.69	1.65
Core mass		30.97	18.31	66.83	71.45
Mass loss		8.92	15.12	4.63	5.22
Mass loss % of core		29.0	83.0	7.0	7.0

PUR, polyurethane; PIR, polyisocyanurate.

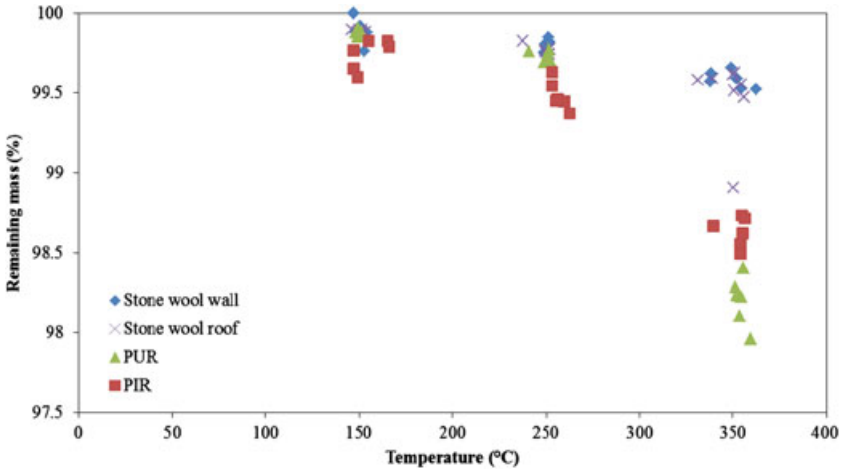

Figure 10. The total mass of the core during the mass-loss experiments at different temperatures. [Colour figure can be viewed at wileyonlinelibrary.com]

The stone wool samples lost approximately 7% of their mass, of which a significant (3% assumed) part could be assigned to the adhesive layer that binds the facing to the core material. The material showed discolourations at high temperatures (Figure 11) and loses strength. The PIR panel lost 29% mass of its core; the tested samples contained an adhesive layer. The samples exposed to temperatures larger than 250 °C expanded due to the formation of a honeycomb structure (a larger open cell structure). This honeycomb structure protected the remainder of the core material. The PUR samples showed a mass loss of 83% due to the pyrolysis that occurred in the influenced area, at high temperatures. The exposed PUR melted and quickly turned into pyrolysis gas.

The mass loss of the influenced area was significantly higher that the mass loss percentages of the complete samples, which give 0.4% mass loss for stone wool samples, 1.0% mass loss for PIR samples and 1.6% mass loss for PUR samples.

4.3. Visible observations

All materials resisted temperatures up to 150 °C without significant damage or mass loss; the mass loss ranged between 0.9 and 2.0 g. All materials showed no reaction to the heat exposure, except stone wool wall panels, which produced a slight odour while testing. At a temperature of 250 °C, there was a slight difference between the stone wool panels and the foam panels; the foam panels showed small signs of delamination combined with an increasing mass loss of 3.0 up to 3.3 g. After removing the inner steel facing the core materials, it showed discoloured foam; both foams show larger cells within their foam, whereas the stone wool panels did not show any signs of delamination, and a mass loss of 2.4–2.6 g after removing the inner steel facing the adhesive layer showed discolouration.

DOI: 10.1002/fam

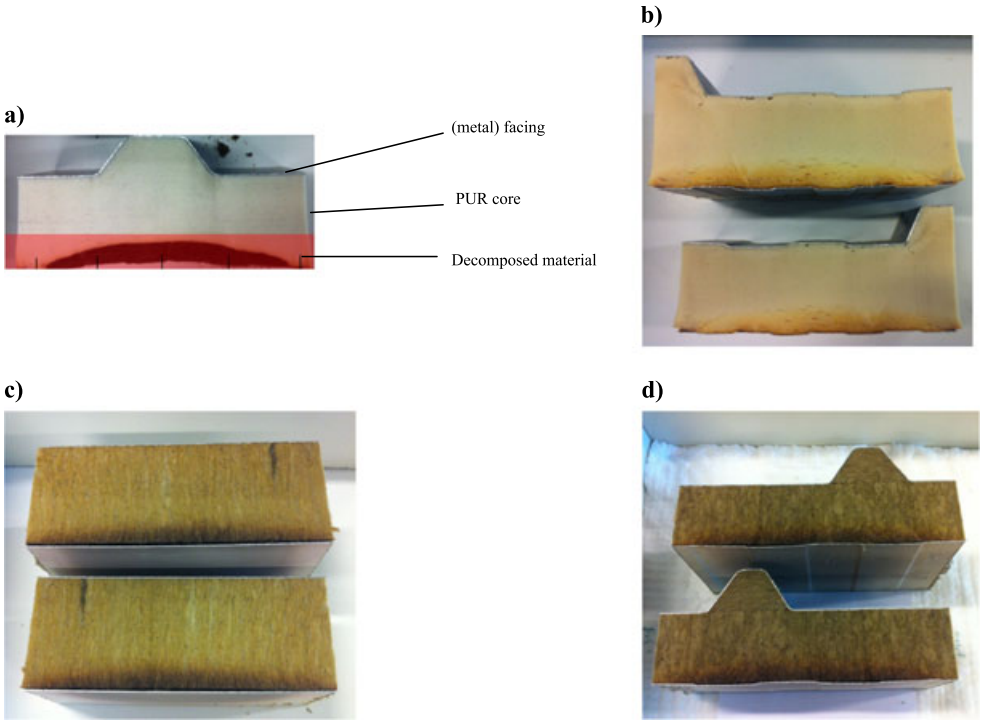

Figure 11. Picture of the decomposition front in (a) polyurethane, (b) polyisocyanurate, (c) stone wool wall and (d) stone wool roof sandwich panel, with red area used for the calculation of the mass loss percentage shown in Figure 11a. [Colour figure can be viewed at wileyonlinelibrary.com]

At temperatures of 350 °C, all panels delaminated and produced smoke. Stone wool panels produced a strong odour of burned glue and showed discolouration of the core material. The PIR panels formed a honeycomb structure, and the PUR panel cores pyrolysed.

4.4. Comparison core and element

There was a difference noticed between the mass loss of a sample exposed from all sides (Section 4.1) and a sample that is exposed to one single side, in accordance with a more realistic fire scenario (Section 4.2). In the realistic scenario, the elevated temperature to which the sample was exposed took more time to migrate through the material when it was exposed to one single side. This showed the importance of testing the material in its applied conditions (i.e. a hot smoke layer inside and an ambient temperature on the outside). It also showed that for insulation materials, the sample size was of importance. The mass loss results from the flammability tests were combined with TGA results from the literature; the difference between both tests is determined by two parameters, namely chemical composition and sample size. Because the temperatures where the mass loss started are comparable for both PUR and PIR, from literature, based on TGA and our experimentally determined mass loss, the most important differences are the sample size and shape. Based on this, it appeared that a greater sample size resulted in improved performance on thermal stability for both PUR and PIR, although the difference in sample composition will also have some effect.

5. ANALYSIS OF FLAMMABILITY OF HOT GASES IN BUILDINGS

In this section, the experimental results from the previous section are used to calculate the flammability of hot gases in buildings, which is of interest for the fire department in order to determine its intervention strategy (offensive fire attack vs defensive fire attack outside the fire compartment). The

DOI: 10.1002/fam

calculation is performed by using a computational model (Section 5.1). The results of the calculations are shown in Section 5.2.

It was not possible to simulate on product level and to do heat transfer simulations. To be able to perform these simulations, more data are needed, provided by the earlier mentioned experiments. The main missing variable for these simulations is the heat resistance coefficients of the material when it changes state due to the exposure of a high temperature and at which temperature the material changes state. Furthermore, it is likely that the heat resistance is depending on the temperature of the insulation material; in order to correctly simulate the heat flow through the insulation material, these variables must be studied first.

5.1. Model

In order to assess the mass loss of insulation materials of a real-size building in the pre-flashover phase, a conventional calculation method is used. By combining Ozone [36] as a two-zone model for fire simulations, with static calculations performed in MSExcel to determine the area of sandwich panels that is exposed to the simulated smoke layer. Ozone is able to simulate realistic fire scenarios according to the natural fire concept. Simulations within Ozone give data about temperature, smoke layer thickness and time. The Excel spreadsheet calculation will use the data output from Ozone of which, time, temperature and smoke layer thickness are the main variables. In Excel, these data from Ozone are used to calculate the area of sandwich panels that is exposed to the smoke layer, as well as the volume of this smoke layer. In the Excel calculations, only the mass loss of the insulation material in relation to temperature and time have been taken into account. For the calculation of the mass loss, the experimental data from Section 4.2 are applied.

The mass loss results of the element experiments (Section 4.2) are used in these calculations as intervals, meaning that the results of the 150 °C test are used for the interval of 100–200 °C, the results of the 250 °C for the interval of 201–300 °C and the results of the 350 °C test for the interval of 301–400 °C. By dividing the exposed area in these temperature intervals, the total mass loss in the pre-flashover phase can be calculated. This is carried out by calculating the mass loss for each data point, adding this cumulative to gain the total mass loss during the fire. In these calculations, all pyrolysed materials will enter the smoke layer. And only the pyrolysed materials of the tested products are taken into account as flammable materials in the smoke layer. So, the mass of the pyrolysis gases generated by the mass loss of the insulation material is combined with the total mass of the smoke layer (the output of Ozone) in order to acquire the concentration of flammable gases comparable with the calculation of the flammability (Eqn (1)). During these simulations, only the pyrolysis gases of the sandwich panels are taken into account. Other materials, for example, from the inventory of the building, that might be pyrolysed are not taken into account.

5.2. Simulation results

In this section, the results of the model of the previous section are described for a single case. More cases can be found in Giunta d'Albani [37]. The cases by Giunta d'Albani [37] are a variety of buildings, which vary in total height, ceiling height, depth, roof angle, pitched roof, single pitched roof, flat roof and opening sizes. The described case is a storage building equipped with the tested roof sandwich panels and double pitched roof. Table VII shows the properties of this storage building. The result of the mass-loss experiments of Section 4.2 is used to calculate the possible total mass loss of a realistic fire scenario (Table VII), using Ozone.

The Ozone simulations contain the material properties of the tested sandwich panels; each simulation uses a different panel type. The different core material properties result in different Ozone data output regarding the smoke layer development (Table VIII). The total mass loss of the PUR panels in the simulated storage building is 325 kg based on the MSExcel calculations (Section 5.1). This mass corresponds with a mass-loss percentage of 3.14% of the total influenced area and a pyrolysis smoke layer ratio of 0.0597 kg/m^3. The PIR panels show a mass loss of 250 kg during the MSExcel calculations, which corresponds with a mass loss of 1.57% of the total influenced area. The smoke layer ratio is 0.046 kg/m^3. The mineral wool roof panels give a total

DOI: 10.1002/fam

Table VII. Properties of the example building and input parameters used in the Ozone fire simulations.

Property	Value
Roof	Double pitched
Floor	Rectangular
Floor area	1500 m^2
Height	8 m
Length	50 m
Depth	30 m
Ceiling height	2 m
Roof angle	7.6°
Openings	None
Fire growth	Medium
RHR	6000 kW/m^2
Fire load	511 MJ/m^2
Floor	15 cm (normal mass concrete (EN1994-1-2))
Ceiling and wall	Sandwich panels conform Table V
Start temperature	20 °C

RHR, rate of heat release.

Table VIII. The results of the simulations when applying the different sandwich panels.

Storage building	PUR	PIR	Stone wool
Mass loss (kg)	325.9	250.2	156.0
Mass loss of influenced area (%)	3.14	1.57	0.74
Pyrolysis gas smoke layer ratio (kg/m^3)	0.06	0.05	0.03
Pyrolysis gas smoke layer ratio (kg/kg)	0.12	0.09	0.05
% pyrolysis mass of total smoke layer mass	11.31	8.2	5.2

PUR, polyurethane; PIR, polyisocyanurate.

mass loss of 152 kg, corresponding to a mass-loss percentage of 0.72% and a smoke layer ratio of 0.027 kg/m^3.

6. CONCLUSIONS

For this research, focussing on the pre-flashover phase of a fire (<400 °C), a special furnace has been designed and built, which has the capability to one-side exposure of sandwich panels and their core materials (stone wool, PUR, PIR, EPS and XPS). The research shows that delamination can occur due to degradation of the resin between metal facings and the core. In case of PUR and PIR, delamination can also occur due to the gasification of the core material.

The mass losses measured in the experiments where the samples were exposed from one side were 7%, 29% and 83% at a temperature of 350 °C for stone wool, PIR and PUR sandwich panels respectively. These values are valid for the visibly damaged area of the samples; the visible intrusion depth of the damage and other results can be found in Table VI. The mass loss of PUR was slowly linearly increasing for temperatures up to 300 °C, but a rapid mass loss occurs from this temperature onwards due to gasification of the PUR core. The mass loss of PIR shows the same course as PUR being stable up to 300 °C but higher mass loss rate from 300 °C and onwards; however, mass loss is lower than PUR. Stone wool panels show a linear mass loss rate throughout the experiment.

Furthermore, the progress of the degradation front at a different temperature was clearly visible when the sandwich panels were cut into two parts.

The flammability ranges for the different insulations core were determined experimentally. The lower and upper flammability ranges for PUR are 9.2 and 74% m/m respectively. A lower flammability for EPS and XPS of 3.1% m/m was found, but during the experiments, the upper limit

DOI: 10.1002/fam

was not found. The effluent of the heating of stone wool and PIR cores could not be ignited during the experiments.

A simulation of a fire event in a storage building, using Ozone, revealed that even in the worst-case scenario, the LFL of 9.2% m/m will be reached by the insulation material (PUR) alone during the pre-flashover phase (<400 °C). Exceeding this LFL is even more likely by a combination of pyrolysis of insulation material and the fire load near the fire in the fire compartment during this phase of a fire. This introduces a risk of a smoke layer explosion, a hazardous situation for the fire brigade in case of an offensive intervention in the fire compartment.

ACKNOWLEDGEMENTS

The authors wish to express their sincere thanks to Brandweer Nederland (Dr Ricardo Weewer), Fellowship FSE WO^2 Foundation (Ir Ruud van Herpen), Kingspan, Rockwool, Stybenex for their materials and technical support and advises. They furthermore thank the sponsors of the user/sponsor group Cement-Immobilisates-Concrete. Furthermore, the authors wish to thank the experts from the field – Roy Weghorst, Benedikt van Roosmaalen, Peter van de Leur and Jacques Mertens – for their input.

REFERENCES

1. Hardwood J, Hume B. Fire safety of sandwich panels, Central Fire Brigades Advisory Council Scottish Central Fire Brigades Advisory Council Joint Committee on Fire Research, 1997. http://www.coldstoremaintenance.co.uk/1997Firesafetyofsandwichpanels.pdf (accessed November 10, 2014).
2. Papadopoulos AM. State of the art in thermal insulation materials and aims for future developments. *Energy and Buildings* 2005; **37**:77–86. doi:10.1016/j.enbuild.2004.05.006.
3. Dakenraad, Dakenmarkt 2015, Dakenmarkt 2015. 2015. http://www.dakenraad.nl/index.php?page=dakenmarkt2015.
4. Hull TR, Stec AA, Lebek K, Price D. Factors affecting the combustion toxicity of polymeric materials. *Polymer Degradation and Stability* 2007; **92**:2239–2246. doi:10.1016/j.polymdegradstab.2007.03.032.
5. Crewe RJ, Stec AA, Walker RG, Shaw JEA, Hull TR, Rhodes J, *et al.* Experimental results of a residential house fire test on tenability: temperature, smoke, and gas analyses. *Journal of Forensic Sciences* 2014; **59**:139–154. doi:10.1111/1556-4029.12268.
6. Alarie YC, Anderson RC. Toxicologic and acute lethal hazard evaluation of thermal decomposition products of synthetic and natural polymers. *Toxicology and Applied Pharmacology* 1979; **51**:341–362. doi:10.1016/0041-008X(79)90476-9.
7. Cooke GME. Resisting collapse of steel-faced sandwich panel walls and ceilings exposed to fire. *Journal of Fire Protection Engineering* 2008; **18**:275–290. doi:10.1177/1042391508087839.
8. Cooke GME. Sandwich panels for external cladding — fire safety issues and implications for the risk assessment process. UK Mineral Wool Association, 2000. http://www.cookeonfire.com/pdfs/Sandwich Panels-Cooke report.pdf.
9. Griffin GJ, Bicknell AD, Bradbury GP, White N. Effect of construction method on the fire behavior of sandwich panels with expanded polystyrene cores in room fire tests. *Journal of Fire Sciences* 2006; **24**:275–294. doi:10.1177/0734904106059052.
10. Stec AA, Hull TR. Assessment of the fire toxicity of building insulation materials. *Energy and Buildings* 2011; **43**:498–506. doi:10.1016/j.enbuild.2010.10.015.
11. Bengtsson LG. *Enclosure Fires*. Swedish Rescue Services Agency: Karlstad, Sweden, 2001.
12. Stec AA, Hull TR, Lebek K, Purser JA, Purser DA. The effect of temperature and ventilation condition on the toxic product yields from burning polymers. *Fire and Materials* 2008; **32**:49–60. doi:10.1002/fam.955.
13. Chattopadhyay DK, Webster DC. Thermal stability and flame retardancy of polyurethanes. *Progress in Polymer Science* 2009; **34**:1068–1133. doi:10.1016/j.progpolymsci.2009.06.002.
14. Singh H, Jain AK. Ignition, combustion, toxicity, and fire retardancy of polyurethane foams: a comprehensive review. *Journal of Applied Polymer Science* 2009; **111**:1115–1143. doi:10.1002/app.29131.
15. Jiao L, Xiao H, Wang Q, Sun J. Thermal degradation characteristics of rigid polyurethane foam and the volatile products analysis with TG-FTIR-MS. *Polymer Degradation and Stability* 2013; **98**:2687–2696. doi:10.1016/j.polymdegradstab.2013.09.032.
16. Jiao L, Xu G, Wang Q, Xu Q, Sun J. Kinetics and volatile products of thermal degradation of building insulation materials. *Thermochimica Acta* 2012; **547**:120–125. doi:10.1016/j.tca.2012.07.020.
17. Vitkauskienė I, MakušKa R, Stirna U, Cabulis U. Thermal properties of polyurethane–polyisocyanurate foams based on poly(ethylene terephthalate) waste. *Materials Science* 2011; **17**. doi:10.5755/j01.ms.17.3.588.
18. Yaws CL. *Matheson Gas Data Book* (7th edn). Matheson Tri-Gas ; McGraw-Hill, Parsippany, NJ: New York, 2001.
19. Racik J. Fire rated insulated (sandwich) panels. *Fire Australia* 2003:33–37.
20. Dominguez-Rosado E, Liggat JJ, Snape CE, Eling B, Pichtel J. Thermal degradation of urethane modified polyisocyanurate foams based on aliphatic and aromatic polyester polyol. *Polymer Degradation and Stability* 2002; **78**:1–5. doi:10.1016/S0141-3910(02)00086-1.

21. Ashida K, Saiki K, Goto J, Sasaki K. Polyisocyanurate Foams Modified by Thermally Stable Linkages, in: Polym. Foams, American Chemical Society, 1997: pp. 81–100. https://doi.org/10.1021/bk-1997-0669.ch006 (accessed November 20, 2014).
22. Dick C, Dominguez-Rosado E, Eling B, Liggat JJ, Lindsay CI, Martin SC, *et al.* The flammability of urethane-modified polyisocyanurates and its relationship to thermal degradation chemistry. *Polymer* 2001; **42**:913–923. doi:10.1016/S0032-3861(00)00470-5.
23. Zhang Y, Shang S, Zhang X, Wang D, Hourston DJ. Influence of the composition of rosin-based rigid polyurethane foams on their thermal stability. *Journal of Applied Polymer Science* 1996; **59**:1167–1171. doi:10.1002/(SICI)1097-4628(19960214)59:7<1167::AID-APP14>3.0.CO;2-2.
24. Gao F, Price D, Milnes GJ, Eling B, Lindsay CI, McGrail PT. Laser pyrolysis of polymers and its relation to polymer fire behaviour. *Journal of Analytical and Applied Pyrolysis* 1997; **40–41**:217–231. doi:10.1016/S0165-2370(97)00044-2.
25. Baker G. Performance of expanded polystyrene insulated panel exposed to radiant heat, Master Thesis, University of Canterbury, 2002. http://ir.canterbury.ac.nz/handle/10092/8474.
26. Zorgman H. De giftigheid van de bij verbranding van polystyreenschuim vrijkomende gassen, TNO, Delft, The Netherlands, 1980.
27. Gurman JL, Baier L, Levin BC. Polystyrenes: a review of the literature on the products of thermal decomposition and toxicity. *Fire and Materials* 1987; **11**:109–130. doi:10.1002/fam.810110302.
28. Karamanos A, Hadiarakou S, Papadopoulos AM. The impact of temperature and moisture on the thermal performance of stone wool. *Energy and Buildings* 2008; **40**:1402–1411. doi:10.1016/j.enbuild.2008.01.004.
29. Sirok B, Blagojevic B, Bullne P. Mineral wool: production and properties, Elsevier, 2008.
30. Balcerowiak W, Gryta M, Kałędkowski B. Thermal stability of binder for mineral wool insulations. *Journal of Thermal Analysis and Calorimetry* 1995; **43**:299–303.
31. Balkevicius V, Christauskas J, Gailius A, Spokauskas A, Siaurys V. Analysis of some properties of model system from low-melting illite clay and fibrous mineral wool waste. *Materials Science — Poland* 2007; **25**:1 .http://yadda.icm.edu.pl/yadda/element/bwmeta1.element.baztech-article-BPW8-0003-0021 (accessed December 16, 2014)
32. Gardziella A, Pilato L, Knop A. Phenolic resins: chemistry, applications, standardization, safety, and ecology, 2000. https://doi.org/10.1007/978-3-662-04101-7 (accessed September 18, 2015).
33. Robbins AP, Wade CA. Effective passive roof venting in the event of a fire; part 1: preliminary modelling results, BRANZ, 2008.
34. Stybenex, Indicatie vlakdak EPS staalsandwich panelen, 2014.
35. Eurocode, Implementing council directive 89/106/EEC as regards the classification on the reaction to fire performance of construction products, 2000.
36. Cadorin JF, Franssen JM, Pintea D. The design fire tool Ozone V2.0—therorethical description and validation on experimental fire tests, 2001. http://dan.ct.upt.ro/fie/OZone_V2.pdf.
37. Giunta d'Albani AW. Fire behaviour of sandwich panel core materials in the pre-flashover phase, *Master Thesis*, Eindhoven University of Technology, 2014.